CHIN. PHYS. LETT. Vol. 38, No. 2 (2021) 027202

Suppressed Thermal Conductivity in Polycrystalline Gold Nanofilm: The Effect of Grain Boundary and Substrate

Lan Dong(董岚)[1†], Xiangshui Wu(吴祥水)[2], Yue Hu(胡跃)[1], Xiangfan Xu(徐象繁)[2*], and Hua Bao(鲍华)[1*]

[1] *University of Michigan-Shanghai Jiao Tong University Joint Institute, Shanghai Jiao Tong University, Shanghai 200240, China*

[2] *Center for Phononics and Thermal Energy Science, China-EU Joint Center for Nanophononics, School of Physics Science and Engineering, Tongji University, 200092 Shanghai 200092, China*

(Received 6 October 2020; accepted 18 November 2020; published online 27 January 2021)

We investigate the electrical conductivity and thermal conductivity of polycrystalline gold nanofilms, with thicknesses ranging from 40.5 nm to 115.8 nm, and identify a thickness-dependent electrical conductivity, which can be explained via the Mayadas and Shatzkes (MS) theory. At the same time, a suppressed thermal conductivity is observed, as compared to that found in the bulk material, together with a weak thickness effect. We compare the thermal conductivity of suspended and supported gold films, finding that the supporting substrate can effectively suppress the in-plane thermal conductivity of the polycrystalline gold nanofilms. Our results indicate that grain boundary scattering and substrate scattering can affect electron and phonon transport in polycrystalline metallic systems.

DOI: 10.1088/0256-307X/38/2/027202

In recent years, there has been a rapid growth in demand for miniaturization in integrated devices. Advances in nanofabrication technology have reduced the structure size of CPU transistors down to 7 nm. Moore's law has been considered invalid since the beginning of the 21st century.[1] One of the reasons for this is that the scaling down of integrated devices produces a great deal of waste heat at nanoscale/microscale, resulting in the formation of "hot spots".[2] Owing to the significant jump in device deactivation and degradation caused by hot spots, thermal management and the regulation of nanoscale materials has become increasingly important. Many studies have focused on thermal management and thermal regulation in nanoscale structures, providing both theoretical and experimental support for research into the thermal transport mechanisms occurring in nanoscale materials.[3–5] The main components of integrating transistors are nanoscale metals and semiconductors. More specifically, nanoscale metals, metal-metal interfaces and metal-semiconductor interfaces coexist in these nanodevices. Therefore, the high speed operation of these devices can potentially produce a large amount of waste heat which requires to be dissipated into the surrounding environment via various interfaces and nanoscale metals. On that basis, a greater understanding of thermal transport mechanisms in nanoscale metals is key to achieving heat dissipation in integrated devices.

With respect to nanoscale metallic structures, previous works have focused predominantly on the discussion of the Wiedemann–Franz law,[6–10] which is commonly used to interpret the relation between the electrical conductivity (σ) and the electronic thermal conductivity (κ_e) of bulk metal.[11] When the size of the metal is comparable to the electron mean free path, the scatterings at sample surfaces and grain boundaries[12–17] become the dominating impediment to electrical transport. At the same time, electron-phonon coupling[18,19] may also affect thermal transport. Therefore, the Lorenz number, L, exhibits a large difference compared with that in bulk metal (Sommerfeld number $\sim 2.44 \times 10^{-8}\,\mathrm{V^2/K^2}$). In addition, a few studies have shown that substrate scattering may also reduce the thermal conductivity of gold film. Notably, Mason and his co-workers measured the in-plane thermal transport of nanograined polycrystalline gold thin film.[20] The gold films were supported by a SiN_x substrate, reducing thermal conductivity by 40%, as compared with that of a suspended film. Lin and co-workers selected a sub-10 nm thin gold nanofilm deposited onto a micro glass fiber, finding that the thermal conductivity of the supported 6.4-nm-thick gold film is only $61.7\,\mathrm{W\cdot m^{-1}\cdot K^{-1}}$, which represented a 60% reduction in thermal transport, as compared with that of a suspended gold film.[21]

The heat dissipation of integrated devices is primarily affected by the heat conduction of the nanoscale metal (in-plane thermal transport) and heat conduction at the interfaces (cross-plane thermal transport). An important question here relates to the role of in-plane thermal transport and inter-

Supported by the National Natural Science Foundation of China (Grant Nos. 51676121 and 12004242).

†Current address: School of Environmental and Materials Engineering, Shanghai Polytechnic University, Shanghai 201209, China

*Corresponding authors. Email: xuxiangfan@tongji.edu.cn; hua.bao@sjtu.edu.cn

© 2021 Chinese Physical Society and IOP Publishing Ltd

facial thermal transport in the thermal conduction of metal nanofilms, and their effect on heat dissipation in nano/micro devices. Li *et al.* analyzed the relationship between the in-plane thermal transport of thin films and the interfacial thermal transport between thin films and substrate in graphene electronic devices. They found that the cross-plane heat flow dominates the thermal dissipation when the device size is in the order of microns, whereas in-plane thermal transport becomes critical to thermal dissipation when the device size is reduced to nanometers, depending on the in-plane thermal conductivity and the interfacial thermal resistance. This indicates that an understanding of in-plane thermal conductivity in nanoscale metals is key to achieving effective heat dissipation. Although there is evidence to show that metal films on the supporting layer may reduce thermal conductivity,[22] to date there has been no systematic investigation of the substrate's effect on the thermal conductivity of metal nanofilms.

In this work, we conducted a systematic experimental investigation into the in-plane thermal transport of supported and sandwiched gold nanofilms. Polycrystalline gold nanofilms were deposited onto a SiN_x beam in the middle of MEMS (micro-electro-mechanical system) devices. The thermal bridge method was applied to characterize the in-plane thermal transport of the gold nanofilms, and the four-probe method was used to measure the electrical transport of the sample. Three gold nanofilms with thicknesses ranging from 40.5 nm to 115.8 nm, and crystallite sizes ranging from 20.0 nm to 27.4 nm were studied, whose thermal conductivity was found to have weak dependence on sample thickness. Furthermore, we fabricated a sandwiched $Al_2O_3/Au/SiN_x$ structure and achieved a further reduction in the thermal conductivity of the polycrystalline gold nanofilm, suggesting that scattering from the substrate dominates the thermal conductivity in supported gold thin films

Experimental Methods and Sample Characterization —Gold Nanofilm Fabrication. High purity gold wire (99.99% pure Au from Kurt J. Lesker) and chromium sheet metal (99.99% pure Cr from Kurt J. Lesker) served as steam sources to deposit polycrystalline gold nanofilms and adhesion layers (5 nm). We selected three gold nanofilm samples of the same length (32 μm) and width (5 μm), but with different thicknesses (No. 1: 40.5 nm; No. 2: 66.3 nm; No. 3: 115.8 nm). A MEMS device with a SiN_x beam across the two thermometers was selected to measure the electrical and thermal transport properties simultaneously, with the SiN_x beam being employed to support the upper gold nanofilm [as shown in Fig. 1(a)]. In order to avoid a short circuit in the thermometers during the course of gold thermal evaporation, we used electron beam lithography (EBL) to expose a rectangular area, including the whole SiN_x beam and four electrodes. These four electrodes are electrically insulated from the two thermometers, and are only used to measure the electrical properties of the gold nanofilm [as shown in Fig. 1(b)]. The polycrystalline gold layer and the chromium adhesion layer can then be atomically deposited over the whole surface of the supported MEMS device (Kurt J. Lesker, Nano 36, thermal evaporation). In addition to the exposed rectangular area mentioned above, no metal atoms could be permitted to remain after the developing process. This is so that the PMMA resistor can selectively protect the unexposed area, and the two thermometers could be electrically insulated from the gold nanofilm.

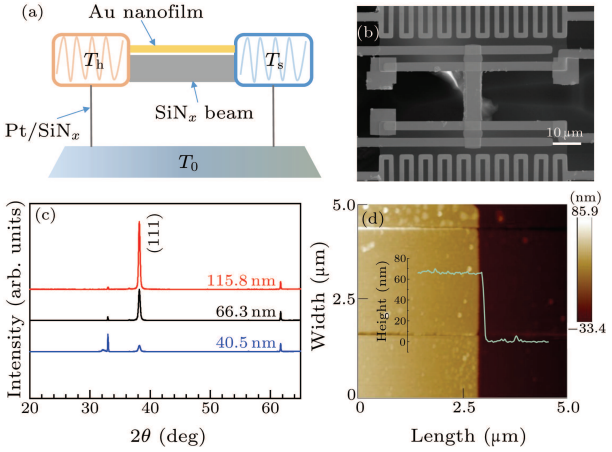

Fig. 1. (a) Schematic diagram of the thermal bridge method used in our experiments; (b) SEM images of the polycrystalline gold nanofilm on the suspended MEMS device, where the inset scale bar is 10 μm; (c) x-ray diffraction results for samples of different thickness. (d) AFM height sensor images of gold nanofilm with a thickness approaching 66.3 nm.

Suspended Sample Preparation. The supported MEMS device was annealed in an H_2/Ar atmosphere at around 250℃ for 2–3 hours prior to the deposition of the gold nanofilm. This annealing pretreatment is used to ensure that no water molecules or polymer residues remain on the surface of the device. The supported MEMS device was pre-processed via micro/nano procedures, including ultraviolet lithography, metal deposition, lift-off and deep reactive ion etching. Having fabricated the polycrystalline gold nanofilm, the MEMS device is then suspended by means of wet etching (30% KOH solution). The suspended MEMS device with polycrystalline gold nanofilm is then analyzed via the following electrical and thermal transport measurements [as shown in Fig. 1(b)].

Morphology Characterization. The size and morphology of the deposited gold nanofilms on the suspended MEMS devices were assessed via scanning electron microscopy (FEI, SEM Nova 450). The thickness of the three suspended gold nanofilms were characterized using an atomic force microscope (Bruker, AFM Dimension EDGE) following the electrical and

thermal measurements. Figure 1(d) shows AFM height image for a gold nanofilm with a thickness approaching 66.3 nm. In order to investigate the crystallinity and the crystallite size of the samples, we deposited the other three wafer-sized gold nanofilms. These three nanofilms were fabricated simultaneously with the suspended gold samples, under the same evaporation conditions, and are used for further x-ray diffraction tests [shown in Fig. 1(c)]. The average crystallite size (D) of the polycrystalline gold nanofilm can be estimated using the well-known Scherrer formula,[23]

$$D = \frac{Ka}{\beta \cdot \cos\theta}, \tag{1}$$

where K is a constant determined by crystallite shape, usually taken as 0.89, a is the x-ray wavelength (0.15419 nm), β is the peak width of the diffraction peak profile at half maximum height, and θ is the diffraction angle. D is calculated to be 20.0 nm, 24.7 nm, and 27.4 nm for the 40.5 nm, 66.3 nm, and 115.8 nm nanofilms, respectively.

Electrical and Thermal Conductivity Measurements. The four-probe method was used to measure the in-plane electrical conductivity of the gold nanofilms, and the traditional thermal bridge method[24–29] was utilized to measure the thermal conductivity of the samples. The electrical and thermal measurements are both based on pretreated suspended MEMS devices. For the electrical measurement, two outer electrodes were designed to add a 1 μA AC current (current source, Keithley 6221) and the other two electrodes were used to measure the corresponding voltage (lock-in amplifier, SRS 830). For the thermal measurement, the temperature gradients at both ends of the gold nanofilms were characterized by two resistive thermometers. The whole suspended MEMS device with gold nanofilm and SiN_x beam was placed into a cryostat with a high vacuum in the order of 1×10^{-4} Pa to reduce the thermal convection.[30] The two thermometers act as heater resistor and sensor resistor, and were employed to characterize the temperature rise (ΔT_h and ΔT_s) at either end of the nanofilm. A combined 1 μA AC current and 70 μA DC current (current source, Keithley 6221) were applied to the heater resistor, with the DC current being used to provide joule heat, and the AC current to observe changes in the resistance of the heater. The same AC current was added to the sensor, and was used to measure changes in the resistance of the sensor.[31,32] The thermal conductance of the gold nanofilm and SiN_x beam could then be calculated by

$$G_b = \frac{Q_{tot}}{\Delta T_h + \Delta T_s}, \tag{2}$$

$$G_{Au+SiN_x} = \frac{G_b \Delta T_s}{\Delta T_h - \Delta T_s}, \tag{3}$$

where Q_{tot} is the total heat flow of the heater, and ΔT_h and ΔT_s represent the temperature increases in the heater and sensor, respectively. Here, G_{Au+SiN_x} represents the total thermal conductance, including the gold nanofilm and the SiN_x beam, and G_b is the thermal conductance of the Pt/SiN_x beams. In order to obtain the thermal conductance of the gold nanofilm, we must measure the thermal conductance of the SiN_x beam separately. Figure 1(a) shows a schematic diagram of the thermal transport measurement process in this experiment. We choose the adjacent suspended MEMS device with a similar thickness of SiN_x beam to measure the thermal conductance of the SiN_x beam. Based on the process mentioned above, the thermal conductivity of the polycrystalline gold nanofilm can be obtained by

$$G_{Au} = G_{Au+SiN_x} - G_{SiN_x}, \tag{4}$$

$$\kappa = G_{Au}\frac{L_s}{A}, \tag{5}$$

where κ is the thermal conductivity of the gold nanofilm, G_{Au} is the thermal conductance of the gold nanofilm, and G_{SiN_x} is the thermal conductance of the SiN_x beam on the adjacent device; L_s and A are the length and cross section area of the gold nanofilm.

Results and Discussion. Figure 2(a) depicts the electrical conductivity of the polycrystalline gold nanofilms with thicknesses ranging from 40.5 nm to 115.8 nm. The electrical conductivity of the three nanofilms decreases as the temperature increases from 40 K to 300 K, which is consistent with the results for bulk gold. As the thickness of the polycrystalline nanofilm decreases, the electrical conductivity also decreases, with the electrical conductivity of the gold nanofilm being far lower than that of bulk gold. These results are in line with previous studies.[13,33]

We then use the Mayadas and Shatzkes (MS) theory[34] to fit the electrical conductivity of the gold nanofilm. In MS theory, electrical conductivity is expressed as $\sigma = \sum_\lambda \sigma_{\lambda,bulk} S_\lambda$, where $\sigma_{\lambda,bulk}$ denotes the bulk thermal conductivity of electron mode λ; S_λ denotes the "suppression function" for electrons, which records the size dependence of the electrical conductivity. For the thin film, S_λ is expressed as

$$\begin{aligned} &S_\lambda(H, D, \tau_\lambda, v_\lambda, p, R) \\ =&\frac{\tau'_\lambda}{\tau_\lambda}\frac{1}{H}\int_0^H \Big[1 - \frac{1-p}{1-p\exp[-H/\tau'_\lambda|v_{y,\lambda}|]} \\ &\cdot \exp\Big(-\frac{|y-y_B|}{\tau'_\lambda|v_{y,\lambda}|}\Big)\Big]dy, \end{aligned} \tag{6}$$

where τ_λ is the intrinsic relaxation time, v_λ is the electron velocity, H is the thickness of the thin film, and p denotes the diffuse reflection. Here, τ'_λ is the relaxation time considering the intrinsic (electron-phonon scattering) and grain boundary scattering processes, and is expressed as

$$\frac{1}{\tau'_\lambda} = \frac{1}{\tau_\lambda} + \frac{\alpha}{2\tau}\frac{v_\lambda}{|v_{\lambda,x}|}, \quad \alpha = \frac{v_\lambda \tau_\lambda}{D}\frac{R}{1-R},$$

where R is the reflection coefficient, and D is the crystallite size obtained from our x-ray diffraction results [Fig. 1(c)] and the Scherrer formula. Here, D is given as 20.0 nm, 24.7 nm, and 27.4 nm for the 40.5 nm, 66.3 nm, and 115.8 nm gold nanofilms, respectively. The relaxation time, electron velocity, and mode-dependent electrical conductivity are obtained by first-principles calculations, which can found in our previous work.[35,36] Our experimental results agree well with the theoretical results [Fig. 2(a)]. The p for all films is 0. The reflection coefficients are 0.76, 0.25, and 0.18 for the 40.5 nm, 66.3 nm, and 115.8 nm nanofilms, respectively. These values are comparable with those found in previous works.[37–39] Both surface scattering and grain boundary scattering could influence the electrical conductivity of the gold nanofilms, but the main factor is grain boundary scattering. The variation of reflection coefficients indicates that the grain boundary plays different roles in terms of electron scattering in different samples.[40] For samples where R approaches 0, electrons transmit grain boundaries more easily than reflecting them. For samples where R approaches 1, it is more common for electrons to be reflected by grain boundaries.

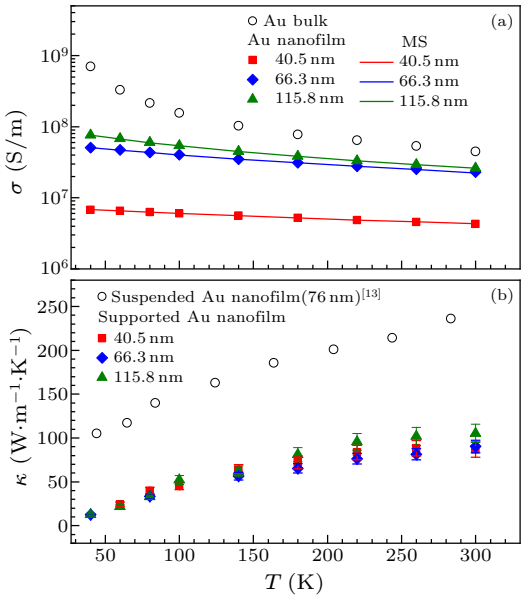

Fig. 2. (a) Thickness-dependent electrical conductivities of gold nanofilms with respective thicknesses of 40.5 nm, 66.3 nm, and 115.8 nm. (b) Temperature-dependent thermal conductivity of gold nanofilms. The black circles represent the thermal conductivity of an Au film from Wang *et al.*[13]

Figure 2(b) presents the increasing thermal conductivity (κ) of the three polycrystalline gold nanofilms in the temperature region from 40 K to 300 K. The thermal conductivity of the three samples are almost the same at lower temperatures, while in the high temperature region, there is some difference in the thermal conductivities of the nanofilms. This discrepancy is probably due to the uncertainty of thermal measurement. In our experiments we have to consider three aspects of uncertainties: systematic errors, caused by the noise fluctuation from the measurement instruments (Keithley 6221, SRS 830, etc.), temperature uncertainty caused by temperature drift within the vacuum environment, and thickness uncertainty in terms of the results of the AFM height sensor images. We consider the contributions of the three uncertainties and give a measurement uncertainty of no more than 10% for our thermal conductivity measurements. The calculation of measurement uncertainty can be found in our previous work.[28] In contrast to electrical conductivity, there is a weak size effect in terms of the thermal conductivity of polycrystalline gold nanofilms. In the gold nanofilms, electrons and phonons both participate in heat transfer, with the electrons playing an important role in the total thermal conduction of the gold nanofilm. The surface scattering and grain boundary scattering of electrons serve as the main factors affecting the in-plane thermal transport of the nanoscale metal system. The surface of the evaporated gold nanofilm has a certain roughness, which could be considered as a diffusive reflection as mentioned in relation to electrical transport. We assume that the sample surface has the same diffusive reflectance, as compared to that in bulk gold. Therefore, the surface scatterings of nanofilms and bulk gold are similar, and the grain boundary scattering should be considered and used to explain the thickness effect of in-plane thermal transport.

It is worth noting that the electrons reflected from the grain boundaries could transfer heat energy to the phonons on the grain boundaries.[21] This electron-phonon interaction partially increases the heat transfer channels. Electrons reflected back from the grain boundaries cannot contribute to electrical conductivity, but heat energy transferred to the phonons could promote phonon transport and phonon-electron interaction, which enhances the contribution of in-plane thermal conductivity in polycrystalline gold nanofilms. This is probably the reason for the breakdown of the Wiedemann–Franz law in relation to thin metal films. Similar thermal transport mechanisms have been found in polycrystalline platinum nanofilms, as noted in previous works, i.e., the thermal conductivity demonstrates an obvious correlation with size for film thicknesses smaller than 30 nm. However, when the film thickness is in the range from 40 nm to 63 nm, almost identical thermal conductivities in platinum nanofilms can be found (see Ref. [14]). In addition, we find that the trend of thermal conductivity of gold nanofilms in relation to temperature is quite different from that of bulk gold. This increasing thermal conductivity with temperature in the high temperature region is due to the polycrystalline property of the evaporated gold nanofilms. Similar thermal transport behaviors have been reported in other nanoscale metals, such as Ni nanowires[10] and sliver

nanowire.[41,42] Both results demonstrate that grain boundary scattering is the main factor in restraining thermal transport in nanoscale metal structures without substrates.

Table 1. Thickness, crystalline size, thermal conductivity and preparation method of gold films with different structures.

No.	Structure	Crystallite size (nm)	κ ($W{\cdot}m^{-1}{\cdot}K^{-1}$)	Preparation method
I	Suspended[13]	45.3	230	EB-PVD
II	Suspended[16]	23.0	160	EB-PVD
III	Supported film[20]	28.0	94	Thermal evaporation
IV	Supported film (this work)	27.4	105	Thermal evaporation
V		24.7	90	Thermal evaporation
VI		20.0	87	Thermal evaporation
VII	Supported film[21]	11.2	61.7	Not applicable
VIII	Sandwiched structure (this work)	20.0	53	Thermal evaporation

As mentioned above, with a decrease in the thickness of the gold nanofilm from 115.8 nm to 40.5 nm, the electrical conductivity sharply decreases. Moreover, the thermal conductivity of our gold film is not only lower than that of bulk gold, but also lower than that of the suspended gold film demonstrated in a previous work.[16] Table 1 shows the crystallite size, thermal conductivity, and preparation method of Au films fabricated with different structures. The suspended gold films with grain sizes ranging from 45.3 nm to 23.0 nm exhibit reduced thermal conductivity in relation to grain size. As the grain size of the suspended Au film decreases, the thermal conductivity decreases from 230 $W{\cdot}m^{-1}{\cdot}K^{-1}$ to 160 $W{\cdot}m^{-1}{\cdot}K^{-1}$,[13,16] resulted from grain boundary scattering. However, the thermal conductivities in supported Au films hold much lower values comparing to that of suspended ones. We contrast the thermal conductivity of the supported gold films in Mason's work[20] and our results with similar grain sizes of around 20–30 nm fall within the range from 87 $W{\cdot}m^{-1}{\cdot}K^{-1}$ to 105 $W{\cdot}m^{-1}{\cdot}K^{-1}$. Our results are therefore shown to be in good agreement with Mason's results.

Compared with these results, when the grain size is similar (No. II & No. V in Table 1), the thermal conductivity varies by 43%. The difference between these two films is that the No. II film is free standing, whereas the No. V film is supported by a SiN_x substrate. We therefore suggest that the thermal conductivity of gold nanofilms can be suppressed by the substrate underneath. The influence of the supporting layer on the in-plane thermal conductivity of thin films has been fully verified in two-dimensional materials, particularly in relation to graphene, where the in-plane thermal conductivity exhibits a slight increase with thickness due to the suppression of phonon vibrations.[43,44] There are also several works presenting the reduced thermal conductivity of metal films with supporting layers;[20,21] the contribution of substrates to in-plane thermal transport requires further exploration.

To verify the effect of the supporting layer on in-plane thermal transport in gold nanofilms, we fabricated a sandwiched structure in which the gold nanofilm is supported by two supporting layers. Atomic layer deposition (ALD) was used to grow a layer of Al_2O_3 with a thickness of 20 nm on the top surface of a gold nanofilm with a thickness of 40.5 nm, from which a sandwiched structure Al_2O_3/Au nanofilm/SiN_x beam was fabricated. Figure 3(a) shows the thermal conductivity of the 40.5 nm gold nanofilm, before and after the growth of the Al_2O_3 layer. Thermal conductivity decreases across the whole temperature range subsequent to the growth of the Al_2O_3 layer. This reduction phenomenon definitively proves that the supporting layer clearly suppresses the in-plane thermal conductivity of the polycrystalline gold nanofilm.

Figure 3(b) lists the in-plane thermal conductivity of gold films with similar thicknesses, drawn from various works. The bulk Au exhibits the highest thermal conductivity of more than 300 $W{\cdot}m^{-1}{\cdot}K^{-1}$ (green column). The reduced thermal conductivity of the free standing Au film (red column) in Ref. [16] is due to grain boundary scattering on electrons, where the crystalline size of the film is of the same order as the mean free path of electrons. Further reduced thermal conductivity is found in supported Au films (blue columns). We find that the crystalline size of the supported film (20 nm) and the suspended film (23 nm) are almost the same, indicating the same grain boundary scattering, while the in-plane thermal conductivity exhibits a large difference. This suppressed thermal transport is due to the fact that cross-plane scattering could affect the in-plane thermal transport in nanoscale metal systems. To further test the effect of the supporting layer, we select one supporting gold film with 20 nm crystalline size to fabricate the sandwich structure (with two supporting layers). We find that the sandwiched structure has the lowest thermal conductivity (black column). The results show that when the crystalline size is constant, the thermal conductivity of the gold film exhibits a further decrease due to scattering from the supporting layer. Support

layers can therefore significantly inhibit the in-plane thermal transfer of nanoscale metals.

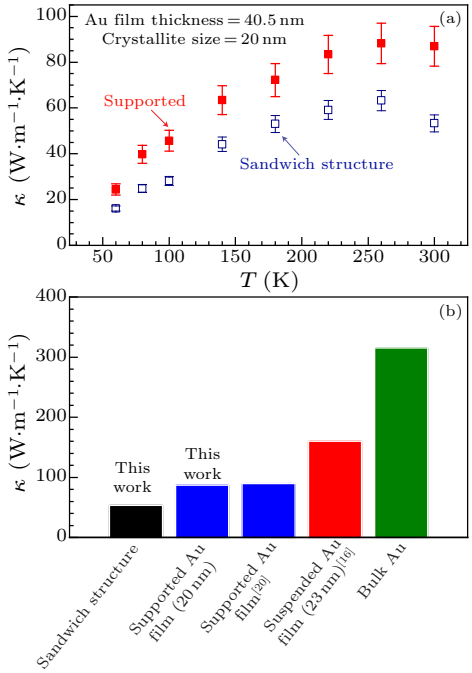

Fig. 3. (a) Thermal conductivity measurement of 40.5 nm gold nanofilm before and after the growth of Al_2O_3. Suppressed thermal conductivity can be observed across the whole temperature range. (b) The influence of support layers on in-plane thermal conductivity of gold nanofilms. The black column represents the sandwich structure used in this work; the two blue columns represent the Au films supported by one layer in our work (crystallize size of 20 nm) and in Mason's work;[20] the red column represents the suspended Au film with a 23 nm crystalline size utilized in Zhang's work.[16]

To conclude, the electrical and thermal conductivity of polycrystalline gold nanofilms with different thicknesses (No. 1: 40.5 nm; No. 2: 66.3 nm; No. 3: 115.8 nm) have been characterized in this work. We have found that electrical conductivity decreases as the thickness of gold nanofilms decreases, which can be fully understood via the MS theory. However, as the thickness of gold nanofilms decreases, there is no obvious size effect in terms of thermal conductivity. Our results also demonstrate that the substrate, along with the grain boundary, affect electronic thermal transport, and are responsible for the reduction in thermal conductivity.

References

[1] Waldrop M M 2016 *Nature* **530** 144
[2] Franklin A D 2015 *Science* **349** aab2750
[3] Zeng Y J, Wu D, Cao X H, Zhou W X, Tang L M, Chen K Q 2020 *Adv. Funct. Mater.* **30** 1903873
[4] Zhou W X, Cheng Y, Chen K Q, Xie G, Wang T and Zhang G 2020 *Adv. Funct. Mater.* **30** 2070048
[5] Hussein M I, Tsai C N and Honarvar H 2020 *Adv. Funct. Mater.* **30** 1906718
[6] Avery A D, Mason S J, Bassett D, Wesenberg D and Zink B L 2015 *Phys. Rev. B* **92** 214410
[7] Zhang X, Zhang Q, Cao B, Fujii M, Takahashi K and Ikuta T 2006 *Chin. Phys. Lett.* **23** 936
[8] Zhang X, Xie H, Fujii M, Ago H, Takahashi K, Ikuta T, Abe H and Shimizu T 2005 *Appl. Phys. Lett.* **86** 171912
[9] Yao M, Zebarjadi M and Opeil C P 2017 *J. Appl. Phys.* **122** 135111
[10] Ou M N, Yang T J, Harutyunyan S R, Chen Y Y, Chen C D and Lai S J 2008 *Appl. Phys. Lett.* **92** 063101
[11] He G, Lu H, Dong X, Zhang Y, Liu J, Xie C and Zhao Z 2018 *RSC Adv.* **8** 24893
[12] Feng B, Li Z and Zhang X 2009 *Thin Solid Films* **517** 2803
[13] Wang H, Liu J, Zhang X and Takahashi K 2013 *Int. J. Heat Mass Transfer* **66** 585
[14] Zhang Q, Cao B, Zhang X, Fujii M and Takahashi K 2006 *J. Phys.: Condens. Matter* **18** 7937
[15] Wang H, Liu J, Zhang X, Guo Z and Takahashi K 2011 *Heat Mass Transfer* **47** 893
[16] Zhang Q, Cao B, Zhang X, Fujii M and Takahashi K 2006 *Phys. Rev. B* **74** 134109
[17] Sawtelle S D and Reed M A 2019 *Phys. Rev. B* **99** 054304
[18] Ma W, Wang H, Zhang X and Wang W 2010 *J. Appl. Phys.* **108** 064308
[19] Wang L, Saira O, Golubev D and Pekola J 2019 *Phys. Rev. Appl.* **12** 024051
[20] Mason S J, Wesenberg D J, Hojem A, Manno M, Leighton C and Zink B L 2020 *Phys. Rev. Mater.* **4** 065003
[21] Lin H, Xu S, Li C, Dong H and Wang X 2013 *Nanoscale* **5** 4652
[22] Li X, Yan Y, Dong L, Guo J, Aiyiti A, Xu X, Li B 2017 *J. Phys. D* **50** 104002
[23] Monshi A, Foroughi M R and Monshi M R 2012 *World J. Nano Sci. Eng.* **02** 154
[24] Xu X, Pereira L F, Wang Y, Wu J, Zhang K, Zhao X, Bae S, Bui C T, Xie R, Thong J T, Hong B H, Loh K P, Donadio D and Li B O B 2014 *Nat. Commun.* **5** 3689
[25] Shi L, Li D, Yu C, Jang W, Kim D, Yao Z, Kim P and Majumdar A 2003 *J. Heat Transfer* **125** 881
[26] Kim P, Shi L, Majumdar A and McEuen P L 2001 *Phys. Rev. Lett.* **87** 215502
[27] Aiyiti A, Hu S, Wang C, Xi Q, Cheng Z, Xia M, Ma Y, Wu J, Guo J, Wang Q, Zhou J, Chen J, Xu X and Li B 2018 *Nanoscale* **10** 2727
[28] Dong L, Xi Q, Chen D, Guo J, Nakayama T, Li Y, Liang Z, Zhou J, Xu X and Li B 2018 *Natl. Sci. Rev.* **5** 500
[29] Aiyiti A, Bai X, Wu J, Xu X and Li B 2018 *Sci. Bull.* **63** 452
[30] Wang Q, Liang X, Liu B, Song Y, Gao G and Xu X 2020 *Nanoscale* **12** 1138
[31] Dong L, Xi Q, Zhou J, Xu X, Li B 2020 *Phys. Rev. Appl.* **13** 034019
[32] Dong L, Xu X and Li B 2018 *Appl. Phys. Lett.* **112** 221904
[33] Zheng P and Gall D 2017 *J. Appl. Phys.* **122** 135301
[34] Mayadas A F and Shatzkes M 1970 *Phys. Rev. B* **1** 1382
[35] Tong Z, Li S, Ruan X and Bao H 2019 *Phys. Rev. B* **100** 144306
[36] Li S, Tong Z, Zhang X and Bao H 2020 *Phys. Rev. B* **102** 174306
[37] Ma W and Zhang X 2013 *Int. J. Heat Mass Transfer* **58** 639
[38] Stojanovic N, Maithripala D H S, Berg J M and Holtz M 2010 *Phys. Rev. B* **82** 075418
[39] Van Attekum P M T M, Woerlee P H, Verkade G C and Hoeben A A M 1984 *Phys. Rev. B* **29** 645
[40] Schneider M A, Wenderoth M, Heinrich A J, Rosentreter M A and Ulbrich R G 1996 *Appl. Phys. Lett.* **69** 1327
[41] Zhao Y, Fitzgerald M L, Tao Y, Pan Z, Sauti G, Xu D, Xu Y Q and Li D 2020 *Nano Lett.* **20** 7389
[42] Cheng Z, Liu L, Xu S, Lu M and Wang X 2015 *Sci. Rep.* **5** 10718
[43] Seol J H, Jo I, Moore A L, Lindsay L, Aitken Z H, Pettes M T, Li X, Yao Z, Huang R, Broido D, Mingo N, Ruoff R S and Shi L 2010 *Science* **328** 213
[44] Jang W, Chen Z, Bao W, Lau C N and Dames C 2010 *Nano Lett.* **10** 3909